LLNL-JRNL-414161

LAWRENCE
LIVERMORE
NATIONAL
LABORATORY

Deep mantle forces and the uplift of the Colorado Plateau

R. Moucha, A. M. Forte, D. B. Rowley, J. X. Mitrovica, N. A. Simmons, S. P. Grand

June 24, 2009

Geophysical Research Letters

Disclaimer

Deep mantle forces and the uplift of the Colorado Plateau

Robert Moucha(1,*), Alessandro M. Forte(1), David B. Rowley(2), Jerry X. Mitrovica(3), Nathan A. Simmons(4), Stephen P. Grand(5)

(1) GEOTOP, Université du Québec à Montréal, Montréal, QC, H3C 3P8, CANADA

(2) The Department of the Geophysical Sciences, University of Chicago, Chicago, IL, 60637, USA

(3) Department of Earth and Planetary Sciences, Harvard University, Cambridge, MA 02138, USA

(4) Atmospheric, Earth & Energy Division Lawrence Livermore National Laboratory, Livermore, California 94551, USA

(5) Jackson School of Geological Sciences, University of Texas at Austin, Austin, Texas 78712, USA

(*) Corresponding author: moucha@sca.uqam.ca

Abstract

Since the advent of plate tectonics, it has been speculated that the northern extension of the East Pacific Rise, specifically its mantle source, has been over-ridden by the North American Plate in the last 30 Myrs. Consequently, it has also been postulated that the opening of the Gulf of California, the extension in the Basin and Range province, and the uplift of the Colorado Plateau are the resulting continental expressions of the over-ridden mantle source of the East Pacific Rise. However, only qualitative models based solely on surface observations and heuristic, simplified conceptions of mantle convection have been used in support or against this hypothesis. We introduce a quantitative model of mantle convection that reconstructs the detailed motion of a warm mantle upwelling over the last 30 Myrs and its relative advance towards the interior of the southwestern USA. The onset and evolution of the crustal uplift in the central Basin and Range province and the Colorado Plateau is determined by tracking the topographic swell due to this mantle upwelling through time. We show that (1) the extension and magmatism in the central Basin and Range province between 25 and 10 Ma coincides with the reconstructed past position of this focused upwelling, and (2) the southwestern portion of the Colorado Plateau experienced significant uplift between 10 Ma and 5 Ma that progressed towards the northeastern portion of the plateau. These uplift estimates are consistent with a young, ca. 6 Ma, Grand Canyon model and the recent commencement of mafic magmatism.

1. Introduction

The Colorado Plateau is part of the Rocky Mountain orogenic plateau bounded by the Basin and Range province to the west and south, the Rio Grande rift and the Great Plains to the east and the southern and central Rocky Mountain orogen to the northeast and north (see Fig. 1a) [e.g. McMillan et al., 2000]. At the end of the Cretaceous the Colorado Plateau, as well as the Great Plains of the USA, was covered by a shallow sea (the Western Interior Seaway).

Today, the Late Cretaceous marine strata of the Western Interior Seaway rest at a mean elevation of about 2 km above sea level atop the Colorado Plateau – thus constraining the amount of post-Cretaceous uplift [Spencer, 1996]. Unlike the Rocky Mountain orogen, there is no evidence of significant crustal shortening for the Colorado Plateau to account for its present-day elevation. Approximately 600 m of the 2 km elevation gain is due to isostatic support of Cretaceous sediments associated with subduction-controlled continental tilting [Mitrovica et. al, 1989] and long-term lithospheric buoyancy may account for an additional 300 m [Spencer, 1996]. The remaining uplift of this region has been the focus of considerable debate, with separate arguments for early-to-middle Cenozoic uplift versus middle-to-late Cenozoic (post 30 Ma) uplift. The early-to-middle Cenozoic uplift of the Western U.S. is generally attributed to a mechanism that modifies, or delaminates, the underlying lithosphere by low angle or "flat slab" subduction of the Farallon plate beneath the North American plate [Bird, 1988; Zandt et al., 1995] or the hydration of the lithosphere by de-watering of the Farallon slab [Humphreys et al., 2003]. In this regard, we note that recent tomographic imaging of mantle structure below La RISTRA seismic array reveals the presence of a warm mantle anomaly underneath the Colorado Plateau [Sine et al., 2008], and this anomaly is interpreted in terms of upward, passive return flow generated by the foundering of the Farallon slab at about 40-20 Ma [Humphreys et al., 2003]. Advocates of middle-to-late Cenozoic tectonic evolution of the Western US Cordillera, including the Colorado Plateau, invoke a mantle plume [e.g. Wilson, 1973; Jacobs et al., 1974; Dixon and Farrar, 1980; Fitton et al., 1991; Parsons et al., 1994]. A recent geodynamic model of present-day flow [Moucha et al., 2008a] driven by density variations derived from a recent, high-resolution seismic tomography model TX2007 [Simmons et al., 2009] demonstrates that the Colorado Plateau currently overlies a strong mantle upwelling. The resulting topographic swell of 500 m coincides well with the physiographic extension of the Colorado Plateau.

There is consensus that the uplift of the Colorado Plateau followed a southwest-to-northeast progression [e.g. Sahagian et al., 2002; McMillan et al., 2006; Flowers et al., 2008; Karlstrom et al., 2008; Polyak et al., 2008]. However, while various paleoaltimetry methods have been utilized to constrain the timing of uplift, little consensus has emerged on this issue. Paleobotanical approaches to paleoaltimetry of the Western US estimate that the Florissant region in the southern Rocky Mountain orogen immediately north of the Colorado Plateau was at its current elevation by 30 Ma [Wolf et al., 1998]. In contrast, paleoelevations derived from vesicular basalts suggest a significant surface uplift (~1.9 km) of the Colorado Plateau that began in the Neogene (25 Ma) and accelerated to present day [Sahagian et al., 2002]. However, this model of recent, rapid uplift has been challenged by Pederson et al. [2002], who invoked an erosional isostasy model to account for the recent uplift the Colorado Plateau.

A recent apatite (U-Th)/He thermochronometry study [Flowers et al., 2008] infers a complex history of regional uplift and denudation associated with rock uplift across the southwestern Colorado Plateau. Surface uplift is inferred from km-scale incision of northeast flowing early to mid (>28Ma) Tertiary drainages across the rim and westernmost interior of the Colorado Plateau. Subsequent drainage reversal led to significant denudation of this part of the Colorado Plateau in late mid and late Tertiarty (<10 Ma) but the relationship to rock uplift is less clear. Estimates of Grand Canyon incision rates and relative vertical displacement across Neogene faults of the Colorado Plateau-Basin and Range transition support a younger than 6 Ma Grand Canyon and a recent uplift of the Colorado Plateau [Karlstrom et al., 2008]. Similarly, erosional isostasy modeling that utilized a younger datum and a larger area than Pederson et al. [2002] also suggest that the Colorado Plateau experienced an uplift of up to 750 m in the last 8 Myrs [McMillan et al., 2006].

2. Tomography Based Mantle Flow Model

In this study we directly address this ongoing controversy by modeling the temporal evolution of mantle flow with a focus on the southwestern US. We quantify its effect on surface topography over the last 30 Myrs, in particular, the onset of uplift of the Colorado Plateau and adjacent regions. We present results from a global time-dependent numerical model of topography that is supported by convectively maintained vertical stresses generated by viscous-flow in the mantle (henceforth termed dynamic topography). These vertical stresses originate from buoyancy forces residing in both the lithosphere and the mantle. The globally distributed present-day mantle and lithospheric density variations are inferred from joint seismic-geodynamic inversions that include mineral physical constraints on the scaling of seismic-shear wave speed to density [Simmons et al., 2009]. A significant result of the joint seismic-geodynamic inversions is that the inferred scalings vary in all three dimensions and thus contain the crucially important effects of intrinsic changes in mantle chemistry and possible partial melting on density. These effects yield cratonic roots with near-neutral buoyancy and reductions of buoyancy in anomalously hot regions in the shallow mantle. The final density model, termed TX2007, provides an excellent fit to present-day geodynamic observables while preserving excellent fit to global seismic data. Specifically, the mantle convection simulation driven by this model yield a fit to the observed free-air gravity, residual topography, and plate divergence (up to spherical harmonic degree 16) to a variance reduction of 90%, 94%, and 76%, respectively. The seismic travel time constraints are satisfied to within 96%.

The convection simulation incorporates Newtonian rheology with a viscosity profile that is constrained by global joint inversions of convection-related surface observables and data associated with the response of the Earth to ice-age surface mass loading [Mitrovica and Forte, 2004]. This profile is labeled 'V1' (Fig. 2d). Since the evolution of dynamic topography is sensitive to adopted viscosity profile, we consider a second viscosity profile that has also been shown to fit geodynamic and ice age observations. 'V2' is shown in Fig. 2c. Compared to V1, this second viscosity model is distinguished by a stiffer lithospheric mantle, a lower asthenospheric viscosity, the absence of a low viscosity notch at the base of the upper mantle, and a stiffer lower mantle (below 2000 km depth).

3. Evolution of Southwestern US Dynamic Topography and Mantle Flow

The time-dependent reconstruction of dynamic topography is obtained via "backward" global mantle convection simulations. We adopt the approach used in Moucha et al. [2008b] where the direction of buoyancy-induced flow in the mantle is numerically reversed by using negative time. To this end, the initial (present-day) temperature distribution is advected backwards using boundary conditions that are consistent with a new Indo-Atlantic plate reconstruction model in the no-net-rotation reference frame. Details of the numerical method can be found in Moucha et al. [2008b]. The inherently high resolution (~100 km) of our global geodynamic model enables us to quantify the role of mantle convection in the evolution of tectonic settings such as the southwestern US.

Fig. 1 depicts the evolution of the southwestern US dynamic topography relative to 30 Ma at 5 Myr intervals in a fixed North American reference frame. Specifically, only the changes in dynamic topography with respect to 30 Ma are shown, because the surface topography at 30 Ma is unknown. Both present-day and 30 Ma dynamic topography are shown in the supplementary section (Fig. S1). We emphasize that a change in dynamic topography corresponds to tectonic uplift (or subsidence) driven by mantle stresses. We do not include here the effect of rock-uplift driven by surface tectonics such as extension, or other surface effects such as erosion or deposition and their corresponding isostatic adjustments. The presentation of these results only accounts for the extension and tectonic re-organization of the southwestern US by incorporating the motion of individual blocks and regions according to a recent tectonic reconstruction [McQuarrie and Wernicke, 2005] addition to dynamic topography, Fig. 1 also shows the evolution of mantle heterogeneity (temperature variations) and the associated flow field along a radial cross-section that is fixed to the rigid North American plate across the Colorado Plateau and neighboring regions. From the temporal evolution along this cross-section, it is evident that a deep-seated warm mantle upwelling has been overridden by the westward motion of the North American plate in the Indo-Atlantic frame of reference. This mantle upwelling coincides with the location of the northern extension of the reconstructed position of the East Pacific Rise as first proposed by Menard [1960] and others [Wilson, 1973; Jacobs et al. 1974; Dixon and Farrar, 1980; Eaton, 1987; Wilson 1988].

In the fixed North American frame of reference, the northeastward-migrating mantle upwelling was beneath the southwestern coast of the US at about 20 Ma, near the present-day location of Los Angeles (Fig. 1b). At this time, the position of the upwelling also coincided with the past intersection of the Mendocino Transform Fault with the East Pacific Rise (the birth place of the Mendocino and Rivera triple junctions) [Dixon and Farrar, 1980]. According to these calculations, the southwestern coast of California and the Baja Peninsula were uplifted by this mantle upwelling between 20 and 15 Ma, (Fig. 1c). This prediction agrees well with sediments cored from the Patton Ridge, located on the Outer Borderland block of California, that suggest that the ridge was uplifted and possibly exposed at sometime between 20-16 Ma [Marsaglia et al., 2006]. At about 15 Ma, the central Basin and Range began a period of extension and mafic magmatism indicating a possible influx of warm mantle beneath the region [e.g. Fitton et al., 1991; Zandt et al., 1995]. The reconstructed mantle cross-section (Fig. 1c) reveals that the bulk of the warm upwelling mantle was indeed located beneath the central Basin and Range province at this time. As this mantle upwelling propagated eastward, the associated topographic swell began to uplift the southwestern edge of the Colorado Plateau at about 10 Ma with a maximum uplift at about 5 Ma (Fig. 1d-e). This relatively recent increase in topography of the southwestern portion of the Colorado Plateau agrees well with the model of a 6 Myr old Grand Canyon proposed by Karlstrom et al. [2008] as well as the apparent west-to-east tilting of the Colorado Plateau [e.g. Sahagian et al., 2002; McMillan et al., 2006; Flowers et al., 2008; Polyak et al., 2008].

4. Dynamic Topography and the Colorado Plateau

A detailed look at the change in the Colorado Plateau's dynamic topography is shown in Fig. 2. Since 30 Ma, vertical mantle flow has increased the dynamic topography of the Colorado Plateau by over a 1000 m in the south to no less than 600 m in the north (Fig. 2a). In the last 5 Myrs, a west-to-east gradient across the Grand Canyon has emerged due to the eastward progression of the mantle upwelling – the eastern block of the Grand Canyon was uplifted by about 200 m in comparison to the western block (Fig. 2b). This is about half the amount of the uplift estimated from the differences in eastern-versus-western Grand Canyon incision rates [Karlstrom et al., 2008]. The additional amount of uplift required to match this observation may be due to effects on topography that we are not modelling, such as erosional isostasy or lateral viscosity variations (i.e. locally reduced viscosity that may enhance the rate of uplift). Moreover, the eastward progression of the mantle upwelling towards the eastern edge of the Colorado Plateau and the Rio Grande rift region over the last 5 Myrs fits well with recent magmatic activity in this region whose trace element geochemistry suggest a mantle source that is similar to oceanic hotspots [McMillan et al., 2000].

Uncertainties in our geodynamic modeling originate from uncertainties in both the adopted density and mantle viscosity models [*see supplementary information*]. In Fig. 2c, we plot the evolution of the integrated average (over the Colorado Plateau) of dynamic topography for viscosity models 1 and 2 (see Fig. 2d) and two density models – one termed 'TX2007' and the other termed 'TX2009'. The TX2009 density model is essential a damped version of the TX2007 density model [Simmons et al., 2009]. That is, the TX2009 density model is inferred from inversions where the short wavelength mantle structure is more strongly damped. Therefore, the amplitude of the modeled dynamic topography is consequently decreased, as seen in (Fig. 2c).

Comparison of the predicted dynamic topography for the two viscosity models suggests that our predictions are only slightly sensitive to variations in viscosity. The stiffer lithosphere and lowermost mantle of V2 cause both the rate of change as well as the amplitude of dynamic topography to decrease. In effect, these different viscosity models, which are both constrained by the same geodynamic observations, provide an estimate of the potential influence of lateral viscosity variations on our results and they appear to be less than the order of the uncertainties in the density model. It is important to note that this globally constrained convection model that is not tuned to regional observations falls well within the range of current estimates of recent topographic evolution of the southwestern US. The essential ingredient in this successful reconciliation of mantle dynamics and surface geology is a robust mapping of the buoyancy forces and their temporal evolution, hence the importance of the new joint seismic-geodynamic inferences of the 3-D mantle density structure [Simmons et al., 2009].

5. Conclusions

We estimate from the uncertainties of our model (Fig 2c) that the average change in the dynamic topography of the Colorado Plateau is in the range of 400 to 1100 m over the last 30 Myrs and that in the last 5 Myrs the change was 100-300 m. Though modest, the impact of this recent change in dynamic topography may have played an important role in the formation of the Grand Canyon by establishing a 200 m gradient in the flow direction of the Colorado River along the Grand Canyon (Fig 2b). Observations support this predicted gradient [Karlstrom et al., 2008]; however, relating this gradient to surface faulting requires a more detailed investigation. Moreover, our numerically reconstructed path of a warm mantle upwelling throughout the Neogene period also provides compelling support for the idea that the tectonic and magmatic evolution of the southwestern US has been driven by this mantle upwelling enhanced by the positive mantle buoyancy under this region [Menard, 1960; Wilson, 1973; Jacobs et al., 1974; Dixon and Farrar, 1980; Eaton, 1987; Wilson, 1988; Fitton et al., 1991; Parsons et al., 1994]. Indeed, our reconstructed path traces the plate kinematic inference by Dixon and Farrar [1980] of where the intersection of the Mendocino Transform fault with the East Pacific rise would have been located if it were not over-ridden by the North American plate.

ACKNOWLEDGMENTS

Support for RM was provided by the Earth System Evolution Program of the Canadian Institute for Advanced Research (CIFAR) in the form of a postdoctoral fellowship. AMF also acknowledges funding provided by CIFAR, the Canada Research Chair program and by the Natural Sciences and Engineering Research Council of Canada. SPG acknowledges NSF grant EAR0309189. This is GEOTOP-UQAM-McGill contribution number 2009-0011.

Prepared by LLNL under Contract DE-AC52-07NA27344.

References

Bird, P. (1988), Formation of the Rocky Mountains, Western United States: A continuum computer model, *Science, 239*, 1501–1507.

Dixon J. M. and E. Farrar(1980), Ridge subduction, eduction, and the Neogene tectonics of southwestern North America, *Tectonophysics, 67*, 81–99.

Eaton, G. P. (1980), Topography and origin of the southern Rocky Mountains and Alvarado Ridge. *In Continental Extensional Tectonics*, *Geol. Soc. Spec. Publ.*, *28*, 355–369.

Fitton, J. G., D. James, and W.P. Leeman (1991), Basic Magmatism Associated With Late Cenozoic Extension in the Western United States: Compositional Variations in Space and Time, *J. Geophys. Res., 96*, 13,693–13,711.

Flowers, R.M., B. P. Wernicke and K. A. Farley (2008), Unroofing, incision, and uplift history of the southwestern Colorado Plateau from apatite (U-Th)/He thermochronometry, *GSA Bulletin, 120*, 571–587.

Humphreys, E., et al. (2003), How Laramide-age hydration of North America by the Farallon slab controlled subsequent activity in the Western U.S, *International Geology Review*, **45**, 575–595.

Jacobs, J. A., R.D. Russell, and J. T. Wilson (1974) *Physics and geology* (2nd ed. McGraw-Hill Book Co., New York, NY, 1974)

Karlstrom, K. E. et al. (2008), Model for tectonically driven incision of the younger than 6 Ma Grand Canyon, *Geology, 36*, 835-838.

Marsaglia, K. M., A. S. Davis, K. Rimkus and D. A. Clague (2006), Evidence for interaction of a spreading ridge with the outer California borderland, *Marine Geology, 229*, 259-272.

McMillan, M. E., P. L. Heller, and L. W. Wing (2006), History and causes of post-Laramide relief in the Rocky Mountain orogenic plateau, *GSA Bulletin, 118*, 393–405.

McMillan, N. J., A. P. Dickin and D. Haag (2000), Evolution of magma source region in the Rio Grande rift, Southern New Mexico, *GSA Bulletin, 112*, 1582–1593.

McQuarrie, N. and B. P. Wernicke (2005), An animated tectonic reconstruction of southwestern North America since 36 Ma, Geosphere, *1*, 147-172.

Menard, H. W. (1960). The East Pacific Rise, *Science, 132*, 1271 - 1278.

Mitrovica, J. X., C. Beaumont and G. T. Jarvis (1989), Tilting of continental interiors by dynamical effects of subduction, *Tectonics, 8*, 1079–1094.

Mitrovica, J.X. and A. M. Forte (2004), A new inference of mantle viscosity based upon a joint inversion of convection and glacial isostatic adjustment data, *Earth Planet. Sci. Lett., 225*, 177-189.

Moucha, R. et al. (2008a), Mantle convection and the recent evolution of the Colorado Plateau and the Rio Grande Rift valley, *Geology, 36***,** 439-442.

Moucha, R. et al. (2008b) Dynamic topography and long-term sea-level variations: there is no such thing as a stable continental platform, *Earth Planet. Sci. Lett., 271*, 101-108.

Parsons, T., G. A. Thompson and N. H. Sleep (1994), Mantle plume influence on Neogene uplift and extension of the US Western Cordillera?, *Geology, 22*, 83–86.

Pederson, J. L., R.D Mackley and J. L. Eddleman (2002), Colorado Plateau uplift and erosion evaluated using GIS, *GSA Today, 12*, 4–10

Polyak, V., C. Hill and Y. Asmerom (2008), Age and evolution of the Grand Canyon revealed by U-Pb dating of water table-type speleothems, *Science, 319*, 1377–1380.

Sahagian, D., A. Proussevitch and W. Carlson (2002), Timing of Colorado Plateau uplift: Initial constraints from vesicular basalt-derived paleo-elevations. *Geology, 30*, 807–810.

Simmons, N.A., A.M. Forte and S. P. Grand (2009), Joint seismic, geodynamic and mineral physical constraints on three-dimensional mantle heterogeneity: Implications for the relative importance of thermal versus compositional heterogeneity, *Geophys. J. Int.,* (Online Advance Pub.), doi:10.1111/j.1365-246X.2009.04133.x .

Sine, C. R., et al. (2008), Mantle structure beneath the western edge of the Colorado Plateau, *Geophys. Res. Lett.*, *35*, doi:10.1029/2008GL033391.

Sonder, L.J. and C. H. Jones (1999), Western United States extension: How the west was widened, *Annu. Rev. Earth Planet. Sci., 27*, 417–462.

Spencer, J. E. Uplift of the Colorado Plateau due to lithosphere attenuation during Laramide low-angle subduction, *J. Geophys. Res.* **101**, 13595–13609 (1996)

Wilson, J. T. (1988), Convection tectonics: some possible effects upon the Earth's surface of flow from the deep mantle, *Can. J. Earth Sci., 25*, 1199-1208.

Wilson, J.T. (1973), Mantle plumes and plate motions, *Tectonophysics, 19*, 149–164.

Wolfe, J. A.,C.E. Forest and P. Molnar (1998), Paleobotanical evidence of Eocene and Oligocene paleoaltitudes in mid-latitude western North America, *GSA Bulletin*, *110*, 664–678.

Zandt, G., S.C. Myers and T. C. Wallace (1995), Crust and mantle structure across the Basin and Range–Colorado

Figure Captions

Figure 1. Evolution of dynamic topography in the southwestern USA in a fixed North-American reference frame relative to 30 Ma for (a) 25 Ma, (b) 20 Ma, (c) 15 Ma, (d) 10 Ma, (e) 5 Ma, and (f) 0 Ma. Rotations of individual blocks within the fixed North-American reference frame are obtained from tectonic reconstructions [McQuarrie, and Wernicke, 2005]. Results are shown for V1 and the TX2007 density model and relative to dynamic topography at 30 Ma [see *supplementary information, Fig. S1*]. Radial cross-sections of the reconstructed mantle temperature variations from surface to core-mantle-

boundary (CMB) along the line A-B, affixed to the rigid North American plate, are shown on the left for each time frame. Superimposed on these cross-sections are the corresponding mantle flow velocity vectors. The vectors are extracted from global flow field in the mantle's no-net rotation frame of reference along a cross section fixed relative to North America. BR = Basin and Range, CBR = Central Basin and Range, SBR = Southern Basin and Range, SRM = Southern Rocky Mountain orogen, CP = Colorado Plateau, GP = Great Plains, OB = Outer Borderland which contains the Patton Ridge. The Rio Grand rift lies between the CP and the GP.

Figure 2. Change in Colorado Plateau dynamic topography with respect to (a) 30 Ma and (b) 5 Ma in a fixed North American reference frame accounting for the slight rotation of the Colorado Plateau [McQuarrie and Wernicke, 2005]. (c) Evolution of the average dynamic topography in the Colorado Plateau over the last 30 Myrs. The average is an area integral of the change in dynamic topography with respect to 30 Ma for each instant in time. Plotted are the results for two viscosity models shown in (d) that are constrained by joint inversion of geodynamic and glacial isostatic adjustment observations [Mitrovica and Forte, 2004] Also shown are the results for two versions of a density model derived from joint seismic-geodynamic inversions [Simmons et al., 2009]. The TX2009 model is a damped (smoother) version of the TX2007 model [see *supplementary information*].

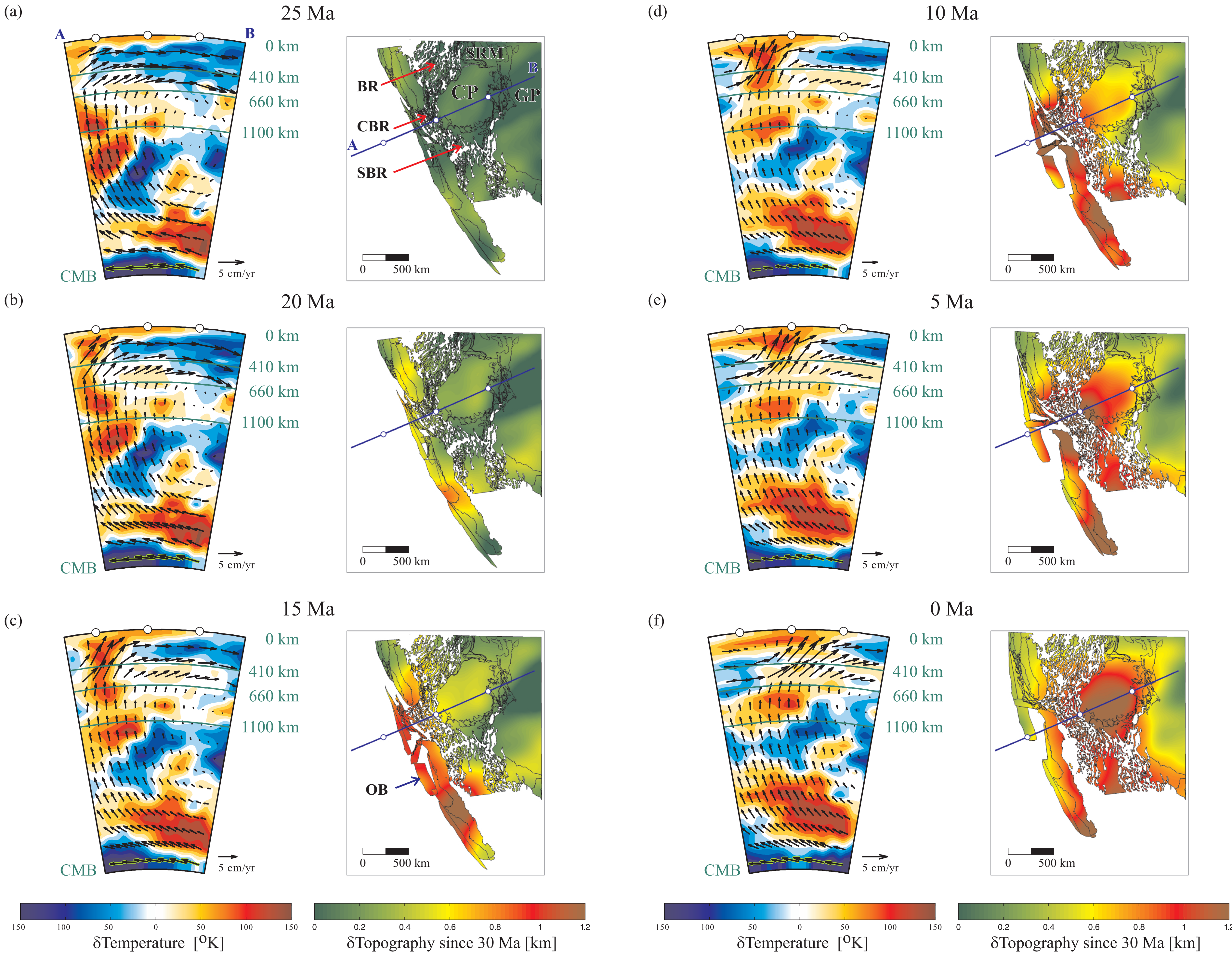
(a)
25 Ma
A
B
0 km
410 km
660 km
1100 km
CMB
5 cm/yr
SRM
BR
CP
GP
CBR
SBR
0
500 km
(b)
20 Ma
(c)
15 Ma
OB
(d)
10 Ma
(e)
5 Ma
(f)
0 Ma
-150
-100
-50
0
50
100
150
δTemperature [°K]
0
0.2
0.4
0.6
0.8
1
1.2
δTopography since 30 Ma [km]

Figure 1.

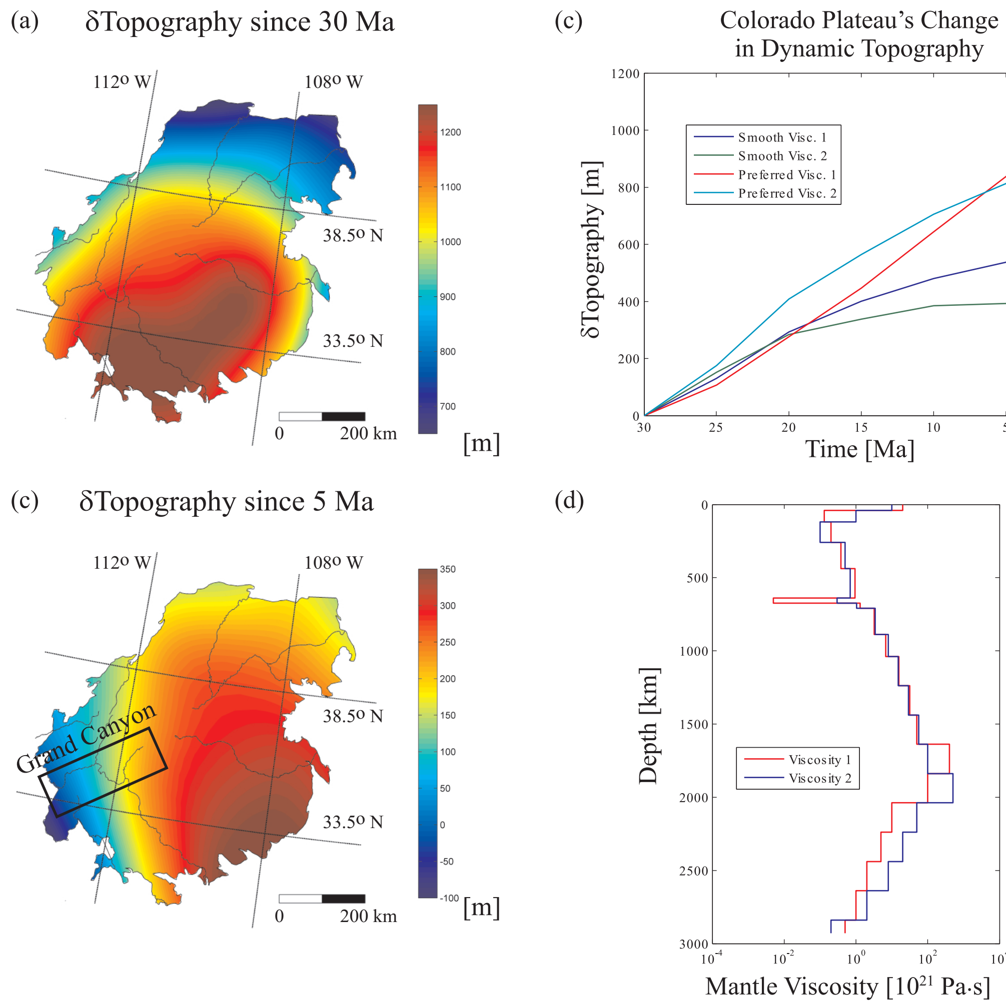

(a)
δTopography since 30 Ma
112o W
108o W
38.5o N
33.5o N
0
200 km
1200
1100
1000
900
800
700
[m]
(c)
Colorado Plateau's Change
in Dynamic Topography
Smooth Visc. 1
Smooth Visc. 2
Preferred Visc. 1
Preferred Visc. 2
δTopography [m]
Time [Ma]
1200
1000
800
600
400
200
0
30
25
20
15
10
5
0
(c)
δTopography since 5 Ma
112o W
108o W
38.5o N
33.5o N
Grand Canyon
0
200 km
350
300
250
200
150
100
50
0
-50
-100
[m]
(d)
Depth [km]
Viscosity 1
Viscosity 2
0
500
1000
1500
2000
2500
3000
Mantle Viscosity [10^21 Pa·s]

Figure 2.

Supplementary Section

Dynamic topography and its rate of change are sensitive to both buoyancy forces used to drive mantle convection and to the adopted viscosity profile. To investigate the effect of mantle rheology on our inferences we use two different viscosity models that are both consistent with mantle convection and glacial isostatic adjustment observations [27]. We label these viscosity profiles as 'viscosity model 1' and 'viscosity model 2'. Overall, the total magnitude of the dynamic topography change is minimally affected by the choice of viscosity model. However, as expected, the rate of change of topography is affected (Fig. 2c), and therefore the reconstructed position and spatial extent of the topographic swell is somewhat different (compare Fig. 2a and Fig. S1a). Also, because of the stiffer lithospheric mantle in viscosity model 2, the magnitude of the west-to-east gradient across the Grand Canyon region is also reduced in comparison to viscosity model 1 (compare Fig. 2b and Fig. S1b). Despite these differences, the total change in dynamic topography since 30 Ma is close to 1000 m regardless of the adopted viscosity model (Fig. 2c).

It is evident in Fig. 2c that, in this case, the choice of density model (inferred from joint seismic-geodynamic inversions [20]) has a greater effect on the calculated uplift of the Colorado Plateau than the viscosity model. The differences between the 'smooth' and the 'preferred' density (or temperature) models are shown in Fig. S2. The amplitude of heterogeneity in the smooth model is considerably less than in the preferred model. As a consequence, the corresponding change in dynamic topography for the smooth model is also less than the preferred model. Nevertheless, the modeled uplift over 30 Myrs in the

Colorado Plateau (Fig. S1c) is still significant fort the smooth model as is the development of a gradient along the Grand Canyon during the last 5 Myrs (Fig. S1d).

Finally, to quantify how much of the uplift is due to deep seated mantle flow, we remove the upper 200 km of mantle heterogeneity from the density model. In Fig. S3 we map the corresponding total dynamic topography change since 30 Ma. On this basis we conclude that the Neogene Colorado Plateau uplift has been driven by a deep seated mantle upwelling that is presently centered beneath the Colorado Plateau.

Supplementary Figure Captions

Figure S1. Change in the dynamic topography within the Colorado Plateau's since (a) since 30 Ma and (b) since 5 Ma predicted using the preferred density model and viscosity model 2. Also shown are analogous results for the smooth density model and viscosity model 1. Compare these results with Fig. 2a-b.

Figure S2. A comparison between present-day mantle temperature variations associated with the smooth and preferred density model derived from joint seismic-geodynamic inversions [20]. The radial cross-section is oriented across the great circle path shown in Fig. S3. Note the reduced amplitudes in the smooth model.

Figure S3. Change in southwestern US dynamic topography over the last 30 Myrs as computed from a model in which the upper 200 km of mantle heterogeneity was removed. Results are shown for viscosity model 1 and for either (a) the smooth density model or (b) the preferred density model.

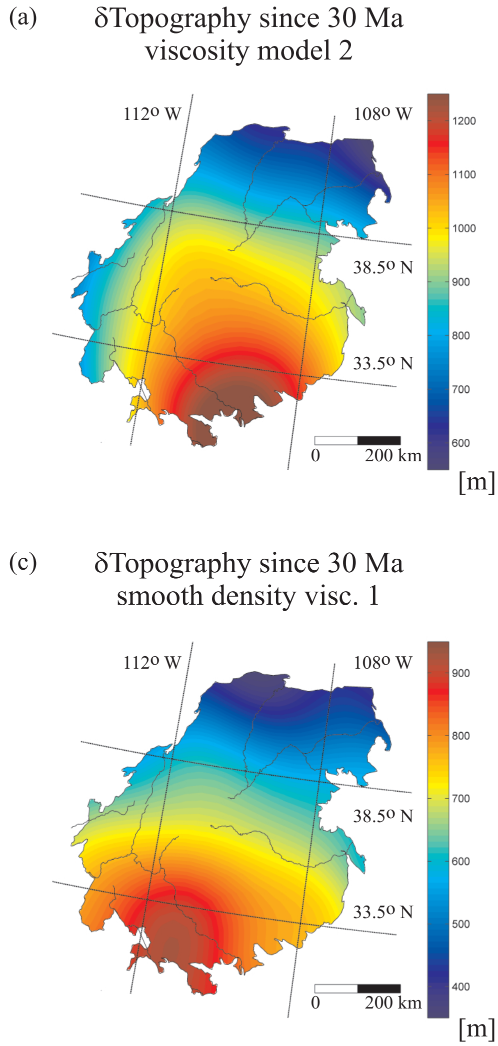
(a)
δTopography since 30 Ma
viscosity model 2
112º W
108º W
38.5º N
33.5º N
0
200 km
1200
1100
1000
900
800
700
600
[m]
(b)
δTopography since 5 Ma
viscosity model 2
112º W
108º W
38.5º N
33.5º N
0
200 km
250
200
150
100
50
0
-50
[m]
(c)
δTopography since 30 Ma
smooth density visc. 1
112º W
108º W
38.5º N
33.5º N
0
200 km
900
800
700
600
500
400
[m]
(d)
δTopography since 5 Ma
smooth density visc. 1
112º W
108º W
38.5º N
33.5º N
0
200 km
250
200
150
100
50
0
-50
[m]

Figure S1.

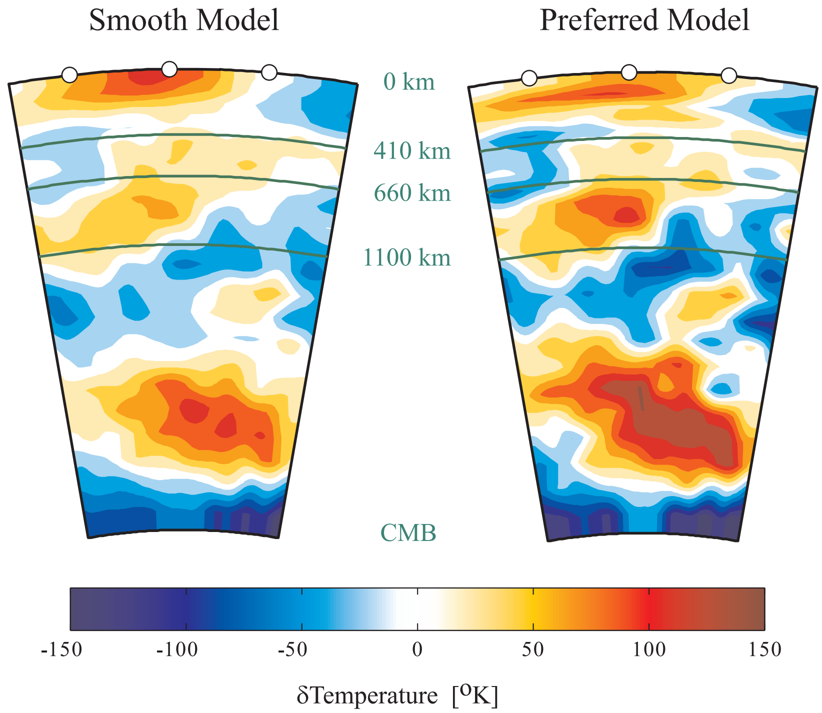

Smooth Model
Preferred Model
0 km
410 km
660 km
1100 km
CMB
-150
-100
-50
0
50
100
150
δTemperature [^{o}K]

Figure S2.

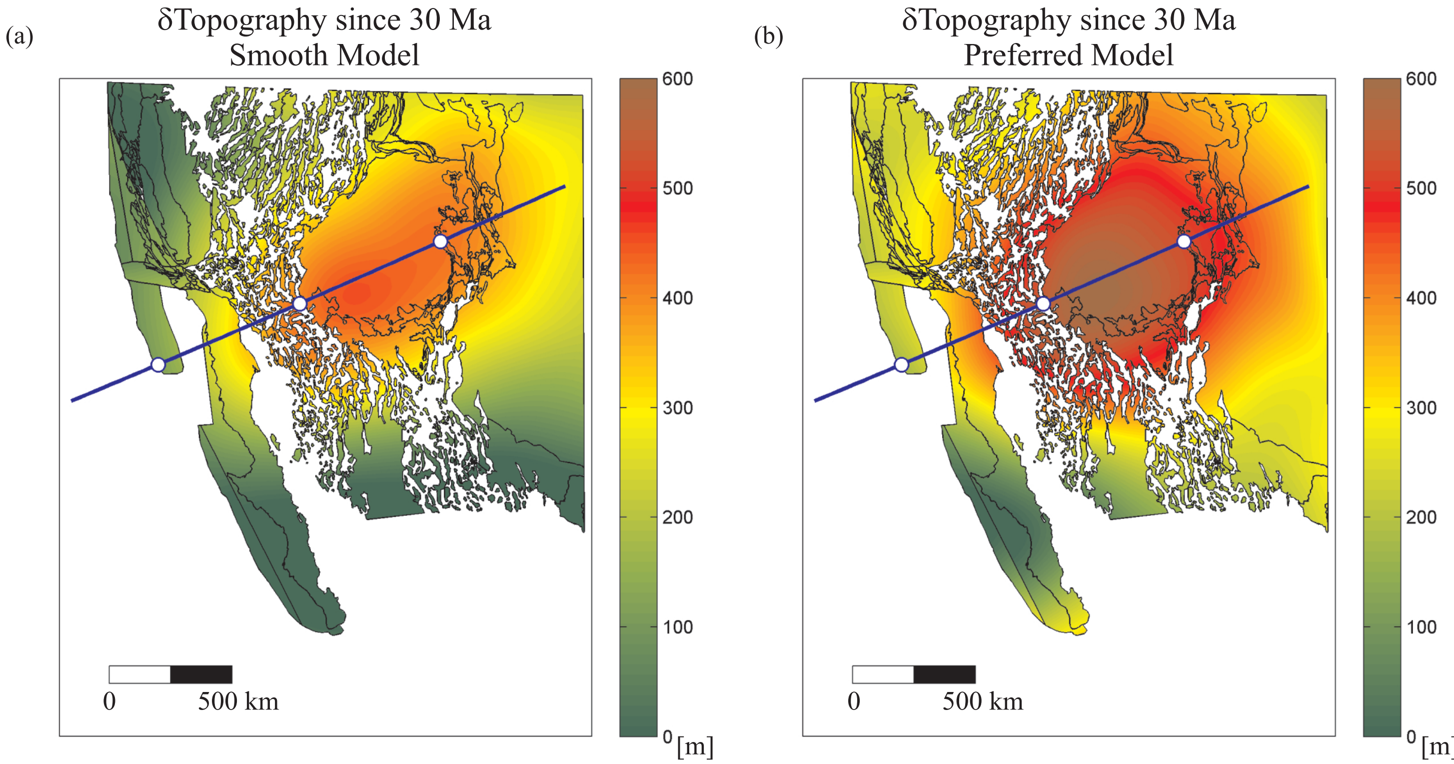
(a)
δTopography since 30 Ma
Smooth Model
600
500
400
300
200
100
0
[m]
0
500 km
(b)
δTopography since 30 Ma
Preferred Model
600
500
400
300
200
100
0
[m]
0
500 km

Figure S3.